

## Free surface tracking with polynomial reconstruction and error correction

Hyoseob Kim<sup>1,\*</sup>,<sup>†</sup>, Byung Soon Jung<sup>1</sup> and Kevin Hall<sup>2</sup>

<sup>1</sup>*Department of Civil and Environmental Engineering, Kookmin University, Seoul, Korea*

<sup>2</sup>*Department of Civil Engineering, Queen's University, Kingston, Ont., Canada*

### SUMMARY

A non-linear method, PREC, for computation of the movement of a free surface is proposed here. The method is composed of three steps: identifying the free surface by using a non-linear function from the volume fraction matrix, updating the volume fraction matrix using a volume projection method with error correction, and treatment of the results using overshooting or undershooting. Identification of the free surface includes using a polynomial function with 2, 4, or 8 coefficients for one-, two-, or three-dimensional problems, respectively. The polynomial reconstruction involves non-negligible numerical error. The second advection step includes a linear projection method in space and time. Advection of the volume fraction matrix is computed from the occupying volume of the mesh at the previous time step. At the new time step, the error at each grid point is assumed to be similar to the error at the previous time step and is used for correction. Overshooting or undershooting develops around the free surface mesh points due to the solution's finite time increment. The third step includes truncating the numerical overshooting or undershooting volumes, i.e. isotropic spreading of the excess fluid volumes. The PREC method is evaluated for a one-dimensional flow case and several two-dimensional simple flow cases with circular sections (cases include transition parallel to a coordinate, transition with an intersection angle to a coordinate, and rotation). The results from the present method are compared with analytical solutions and results from a donor-cell VOF method. As a result of these comparisons, the PREC method is validated. Copyright © 2008 John Wiley & Sons, Ltd.

Received 2 June 2007; Revised 5 December 2007; Accepted 17 February 2008

**KEY WORDS:** finite volume methods; free surface; two phase flows; incompressible flow; differential equations; non-linear solvers

---

\*Correspondence to: Hyoseob Kim, Department of Civil and Environmental Engineering, Kookmin University, Seoul, Korea.

<sup>†</sup>E-mail: hkim@kookmin.ac.kr

Contract/grant sponsor: Kookmin University

Contract/grant sponsor: POSCO E&C

## 1. INTRODUCTION

The computation accuracy of interface movement becomes important when the liquid surface gradient becomes very steep or the surface folds over. For example, simulation of short wave breaking phenomena or the instantaneous wave impact force exerted on a rigid body requires precise tracking of the free surface.

Considering a two-phase problem, often, physical properties show discontinuities, for example, the density, velocity, and pressure gradient vary across the interface boundary, which causes difficulties in the computational approach. The free surface boundary conditions are applied to the interface. A gas or liquid particle on the boundary surface moves with the given flow field surrounding the particle and will therefore stay on the boundary surface unless the boundary surface folds over or attaches to another boundary surface. When a liquid flow has an interface with the open air, a constant atmospheric pressure can be applied along the boundary surface. Different methods for computation of the movement of the free surface have been developed, depending on the numerical techniques or grid systems adopted.

Overall, free surface boundary conditions and the relevant tracking method should include the treatment of the volume, density, flow velocity, and pressure. The interface between an incompressible liquid and a gas in the open space should be considered in addition to the volumetric portion of the free surface.

A wide range of computational methods has been developed to simulate the movement of multi-phase fluids with interfaces. Free surface tracking methods can be classified into different groups (depending on grid structure): grid-free methods, unstructured-grid methods, and structured-grid methods. A typical grid-free method is the smooth particle hydrodynamics (SPH) method proposed by Lucy [1] and others [2, 3]. Several finite element methods or finite difference methods also make use of unstructured grid systems, the form of which may change as computation goes forward.

Methods can also be classified on the basis of movement of the grid positions or particle positions to be computed as moving-grid or Lagrangian methods, and non-moving or Eulerian methods. The moving-grid method has the distinct merit that the computational cell can naturally represent the free surface. The grid-free SPH method introduces fluid particles that contain information on the density, pressure, velocity, and position and can be considered as a Lagrangian method. However, the moving-grid methods allow accumulation of numerical errors due to the distortion of grid system. Some efforts have been proposed to try to reduce the grid-distortion-related total error of the method (see arbitrary Lagrangian–Eulerian method [4]).

Structured-grid methods include both Lagrangian and Eulerian concepts. The Lagrangian methods include the marker-and-cell method [5–7], which is applied to a fixed grid system, but the free surface is tracked in a Lagrangian manner by involving many tracers within a mesh cell. Lagrangian methods have merit in that they guarantee non-diffusive advection of the free surface positions that carry discontinuities of some physical properties across the interface. However, this approach also has several detrimental aspects. First of all, the minimum and maximum number of markers in each surface grid box should be maintained. Other errors are produced in finding new positions of the markers. The position of the final free surface should be found by an interpolation technique from the discrete marker positions with some additional errors.

Eulerian methods include the VOF method [8–16] and level set method [17–19]. A fixed grid method maintains the grid system during computation, and the resolution of the moving interface is one of the key elements for the success of the method. When the grid size is used to

describe the interface between filled and not-filled indication, the resolution of the computation becomes poor. The resolution of these models has been improved by introducing finer description techniques given a coarse grid system. The VOF methods introduce a matrix,  $F$ , an element of which represents volume fraction ratio at each mesh cell and helps describe, indirectly, the shape of the interface, whereas the level set method does not use the volume fraction ratio but uses sophisticated mathematical functions to describe the movement of the interface. Although the level set method can be used to describe highly complex interface geometry, including sharp edges or high curvature, it has difficulty satisfying the conservation of mass principle.

The VOF method solves unsteady convective movement of the index values,  $F$ , so that they may be used in finite difference equations. The  $F$  value at a grid point indicates the volume fraction in a mesh cell. The VOF method has evolved in two different directions since it was proposed by Hirt and Nichols [8]; the geometric reconstruction methods and algebraic interface capturing methods. The algebraic interface capturing methods do not involve geometric reconstruction but use high-resolution advection schemes to compute the VOF matrix [20, 21]. It has been reported that the algebraic methods do not guarantee to suppress numerical diffusion or smearing of the fluid mass and must incorporate some artificial suppression for solution of high-resolution schemes.

If the free surface is expressed as  $z$  in a three-dimensional domain,  $F$  at a grid point  $(i, j, k)$  is

$$F_{i,j,k} = \int_V z_s dV \quad (1)$$

where  $z_s$  is the depth of the fluid in the grid point and  $V$  is the volume.

The  $F$  matrix is considered as discrete values of a conceptual, continuous, and differentiable function in a three-dimensional domain. Matrix  $F$  advects with the following equation:

$$dF(x, y, z, t) = 0 \quad (2)$$

where  $F$  indirectly describes the position of the free surface in a range of  $0 \leq F \leq 1$ . Modifications or refinements of the VOF method have also been proposed by several researchers [22–26].

Inevitable numerical diffusion or smearing of function  $F$ , which includes a transition across the free surface boundary, has been intentionally controlled by suppressing the width of the partial fraction grid points, or chopping and re-distribution of the overflow or underflow volume fraction function around the boundary surface.

Another function,  $f(x, y, z, t)$ , can be defined and used to describe the detailed free surface shape inside a grid point. The detailed function may have either an explicit or an implicit form. Early VOF methods adopted step shapes for the  $f$  function instead of true smooth free surface shapes. More recently, linearly varying or non-linearly varying  $f$  functions have been proposed for higher accuracy [8–12].

The linear improvements of the  $f$  function in the VOF method may take into account either spatial variations or temporal variations of the  $f$  function or both. Kim *et al.* [22] used the following linear relationship between the detailed surface and the other two independent variables for three-dimensional flows and argued that the linear expansion of the detailed free surface description improves the accuracy of the solution in tracking the free surface:

$$z_s = C_1 + C_2x + C_3y \quad (3)$$

where  $z_s$  is the free surface level,  $x$  and  $y$  are the Cartesian coordinates, and  $C_1, C_2, C_3$  are coefficients.

Recently VOF methods using a non-linear  $f$  function have been proposed [23–26]. Kim and No [23] adopted a second-order function to trace the free surface in the  $x$ – $y$  domain:

$$y_s = C_1 + C_2x + C_3x^2 \quad (4)$$

where  $y_s$  is the free surface level in the grid point. The fact that the above method is applicable only to two-dimensional problems is a drawback of the method.

Du *et al.* [24] introduced a polynomial function to express the free surface level in a three-dimensional domain:

$$z_s = C_1x + C_2y + C_3xy + C_4x^2 + C_5y^2 \quad (5)$$

The above equation involves five coefficients that are determined at each time step from minimum number of five surrounding  $F$  values. Furthermore, the required number of  $F$  values varies depending on the distribution condition. A constant coefficient should also be added to the above equation to help express the arbitrary shape of the free surface. When the surface overturns, the above explicit equation for  $z$  should be changed into another explicit equation for  $x$  or  $y$ .

Xiao *et al.* [25] proposed a non-linear  $f$  function in their THINC scheme for tracking the free surface. The function captures the position of the free surface by using the hyperbolic tangent function in each direction instead of the tangent function used in a previous method [26]:

$$f(x) = \frac{C_1}{2} \{1 + C_2 \tanh(C_3(x - x_d))\} \quad (6)$$

where  $x$  is the non-dimensionalized coordinate to the grid size  $\Delta x$ ,  $x_d$  is the non-dimensionalized coordinate of the jump, and  $C_1, C_2, C_3$  are coefficients. The THINC method represents the diffusive feature of a delta function and the derivative function of a step function well. However, the scheme still involves a non-universal parameter, which is selected empirically to account for the direction-dependent behavior of the delta function, and its varying diffusion speed in different directions.

In general, high accuracy is often obtained by sacrificing simplicity or computational efficiency, or *vice versa*. A new relatively simple method for surface tracking, which is still thought to be accurate, is proposed here. This paper concerns the free surface tracking methods for finite difference methods of a regular grid system only. A non-linear distribution of the local volume fraction function,  $f$ , is introduced. Although function  $f$  has a non-linear form, it shows linear variation along each  $x, y$ , or  $z$  direction; in other words, it has a linear form when two independent variables are fixed. The new function is simply defined by the  $F$  matrix around the grid point of interest in one-, two-, or three-dimensional computational domains, depending on the problem.

The new method is tested for simple free surface flow conditions, which have analytical solutions. First, the method is evaluated for pure transition of the free surface in a one-dimensional domain. Second, pure transition of liquid bodies of circular section in a two-dimensional domain with an angle between the bodies of 0–45° relative to a Cartesian coordinate is modelled. Third, rotation of liquid bodies of circular section is evaluated. Test results from the new method are compared with analytic solutions and an early donor cell VOF method.

## 2. THE NEW METHOD, PREC

VOF methods have often been used on a regular grid system. Only two-phase flows are considered here. Wave propagation in a vertical two-dimensional domain is a typical unsteady flow example with a free surface boundary, see Figure 1. As time marches forward, the free surface, which divides air and water, moves across the fixed grid borders.

The matrix element,  $F$ , contains information on the portion of a fluid in a grid point. When the detailed free surface shape at a grid point is known, the exact  $F$  value for the grid point can be determined by integrating the wet depth within the grid point. However, we cannot obtain the detailed surface shape in a grid box from an  $F$  value of the grid box only, which means that the VOF description of the partly filled situation does not provide sufficient information to describe the exact shape of the boundary surface. An  $F$  value defined at the grid center does not provide any information on the center of gravity of the fluid, or the gradient of the surface plane, even if the surface is a plane in the grid box. When the  $F$  arrays are given at grid centers, an infinite number of exact solutions on the free surface shape exist. For example, if  $F$  arrays are given in a two-dimensional domain as in Figure 2, not only straight lines but also many other non-straight curves become solutions. Further assumptions or processes such as interpolation, fitting, or spreading have often been introduced to choose the detailed free surface shape from limited  $F$  array information. Some researchers have used weighting functions that are defined from adjacent

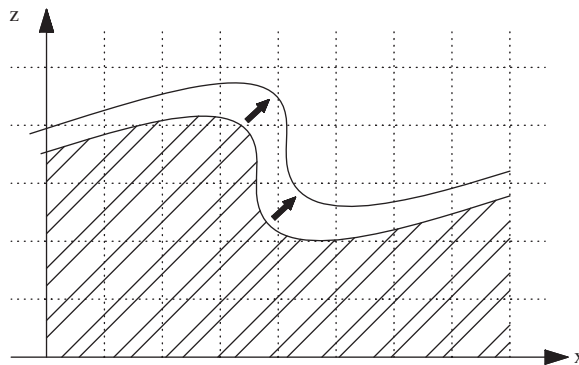


Figure 1. Free surface movement on a regular grid.

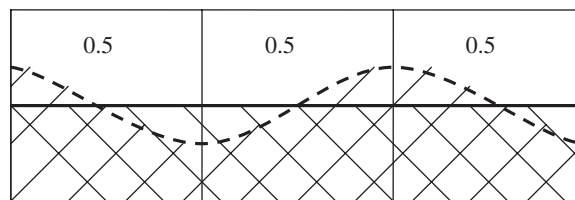


Figure 2. Possible infinite solutions for a given  $F$  array.

$F$  values as a practical choice [7]. This type of approach may tend to produce rather smooth solutions.

A modified algorithm for the existing hyperbolic tangent VOF method [11], to trace the free surface position, is proposed here. The algorithms for velocity and pressure fields, which will complete the whole VOF method, are not dealt with in this paper.

The computation of the  $F$  array with time or tracing the free surface is split into three steps, see Figure 3.

Originally, the VOF method was introduced by converting a discontinuous density distribution into a constant function at a grid point, called  $f$ , which looks like a step function. Ideally, function  $f$  can have a value of 0 or 1 within a grid point. If the step function is expressed by some alternative approximation function, function  $f$  can have a value between 0 and 1, and the precise free surface can be defined as  $f=0.5$  or some other discrete value. The representative volume fraction parameter  $F$  of the grid point and the detailed function  $f$  within the grid point have the same value. An explicit expression for the free surface level can be used instead of an implicit expression like the  $f$  function. In this case, a coordinate to express the free surface needs to be chosen. Consider a simple one-dimensional flow case as that shown in Figure 4. The liquid partly occupies the  $i$ th grid point, attached to the  $(i+1)$ th wet grid point, see Figure 4(a). The derivative of  $f$  in the  $x$  direction is a delta function, see Figure 4(b). However, in order to handle the movement of the delta function in a finite difference scheme, the  $f$  function can take a continuous form instead of being a step function. For example, if the  $f$  function is assumed to be linear between grid centers, as in Figure 4(c), its derivative will have a step function as shown in Figure 4(d). A higher-order or smoother function could be used for  $f$  and its derivative function (see Figure 4(e) and (f) or (g) and (h)). It should be noted that a higher-order function automatically involves more degrees of freedom (or coefficients) in expressing the distribution of  $f$ . Because the physical properties and their derivative function at the free surface have discontinuity or delta function, a higher-order description does not necessarily help solve the problem.

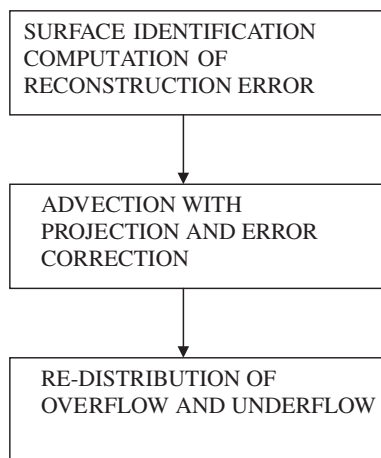


Figure 3. Computation steps of the present method.

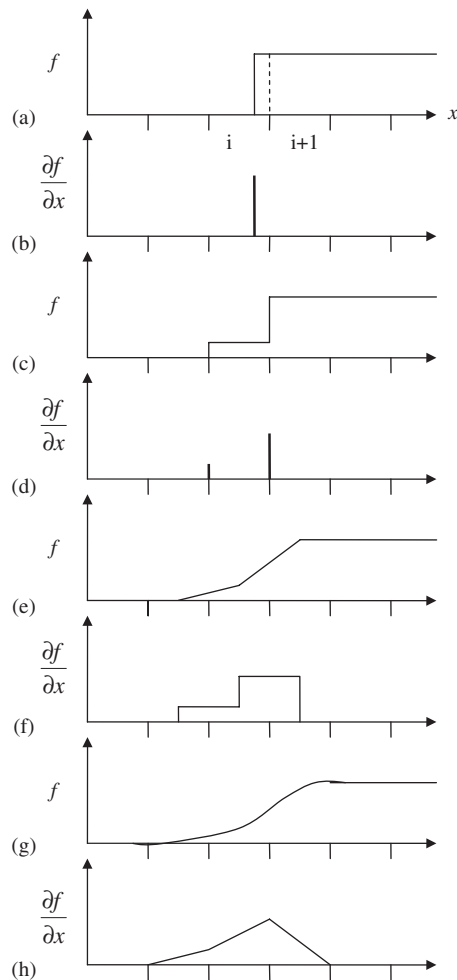


Figure 4. Various concepts of volume-of-fluid and function  $f$ .

The free surface does not physically diffuse, whereas numerical diffusion is inevitable during computation of the advection of the  $F$  array with the VOF method. The numerical diffusion keeps on developing, and reconstruction of the free surface becomes more difficult as time marches forward. Adequate suppression of the numerical diffusion or smearing of the  $F$  array is needed in a VOF method.

A staggered grid system is adopted. It has been widely used for solving flow equations composed of primitive variables such as density, pressure, and velocities. Velocities and fluxes are defined at grid border line centers, whereas the fraction volume array  $F$ , density, and the pressure are defined at grid centers in either three-, two-, or one-dimensional domains. The numbering system of the physical properties in a two-dimensional domain is shown in Figure 5 for convenience.

The first step for identification of the free surface position is important, because it influences the overall accuracy of the surface tracking method. Here a polynomial function is proposed to

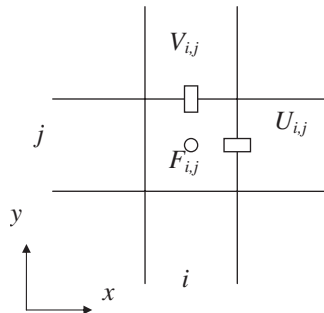


Figure 5. Variables numbering system of the present method.

express a spatially continuous variation of  $f$ , that is

$$\begin{aligned}
 f(x, y, z) &= C_1 + C_2x + C_3y + C_4z + C_5xy + C_6yz \\
 &\quad + C_7zx + C_8xyz, \quad 0 \leq x \leq 1, \quad 0 \leq y \leq 1, \quad 0 \leq z \leq 1 \\
 C_1 &= F_{i,j,k} \\
 C_2 &= F_{i+1,j,k} - F_{i,j,k} \\
 C_3 &= F_{i,j+1,k} - F_{i,j,k} \\
 C_4 &= F_{i,j,k+1} - F_{i,j,k} \\
 C_5 &= F_{i,j,k} - F_{i+1,j,k} - F_{i,j+1,k} + F_{i+1,j+1,k} \\
 C_6 &= F_{i,j,k} - F_{i,j+1,k} - F_{i,j,k+1} + F_{i,j+1,k+1} \\
 C_7 &= F_{i,j,k} - F_{i,j,k+1} - F_{i+1,j,k} + F_{i+1,j,k+1} \\
 C_8 &= -F_{i,j,k} + F_{i+1,j,k} + F_{i,j+1,k} + F_{i,j,k+1} \\
 &\quad - F_{i+1,j+1,k} - F_{i,j+1,k+1} - F_{i+1,j,k+1} + F_{i+1,j+1,k+1}
 \end{aligned} \tag{7}$$

where  $x, y, z$  are non-dimensionalized Cartesian coordinates with respect to the grid sizes in the  $x, y, z$  directions, respectively; and  $F_{i,j,k}, F_{i+1,j,k}, F_{i,j+1,k}, F_{i,j,k+1}, F_{i+1,j+1,k}, F_{i,j+1,k+1}, F_{i+1,j,k+1}, F_{i+1,j+1,k+1}$  are  $F$  values at eight grid centers that compose a cube. Obviously,  $f(0, 0, 0) = F_{i,j,k}$ ,  $f(1, 0, 0) = F_{i+1,j,k}$ ,  $f(0, 1, 0) = F_{i,j+1,k}$ ,  $f(0, 0, 1) = F_{i,j,k+1}$ ,  $f(1, 1, 0) = F_{i+1,j+1,k}$ ,  $f(0, 1, 1) = F_{i,j+1,k+1}$ ,  $f(1, 0, 1) = F_{i+1,j,k+1}$ , and  $f(1, 1, 1) = F_{i+1,j+1,k+1}$ , and the  $f$  function matches well with the  $F$  array.

To have a better view of the  $f$  function, we take a simple two-dimensional example in  $x$ - $y$  domain:  $F_{i,j} = 0, F_{i+1,j} = 1, F_{i,j+1} = 1$ , and  $F_{i+1,j+1} = 1$  (see Figure 6). The three-dimensional view of function  $f$  for the two-dimensional problem within a grid box is shown in Figure 6(a). We define the free surface as the surface where  $f = 0.5$  for the three-dimensional problem, and the contour of  $f = 0.5$  shows the interface curve for the two-dimensional problem, see Figure 6(b).

The new equation for a one-dimensional problem is examined first. A partly filled grid point of (i) ( $F_i = a$ ) is shown in Figure 4(a). Function  $f$  is a piecewise collection of straight lines (see Figure 7).



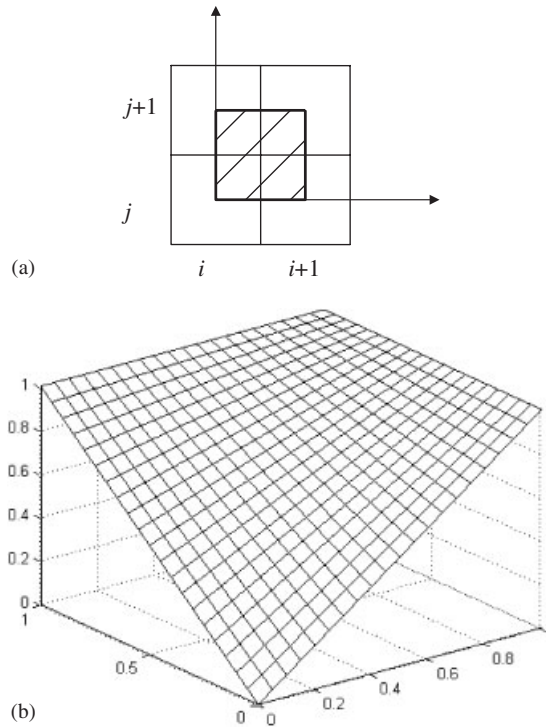


Figure 6. Definition of detailed function  $f$  and example.

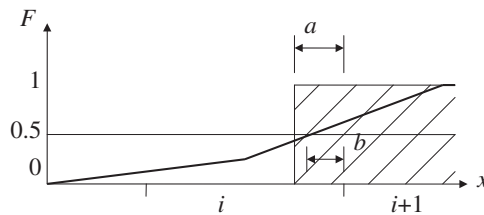


Figure 7. Error produced from polynomial function for one-dimensional flow case.

The simplified equation has the form

$$\begin{aligned}
 f(x) &= C_1 + C_2x, \quad 0 \leq x \leq 1 \\
 C_1 &= F_i \\
 C_2 &= F_{i+1} - F_i
 \end{aligned}
 \tag{8}$$

Finding the surface position from  $f=0.5$ , where the linear  $f$  function crosses a constant level of 0.5, the computed fraction volume of  $F_i^*(=b)$  is not the same as the given  $F_i(=a)$  directly drawn

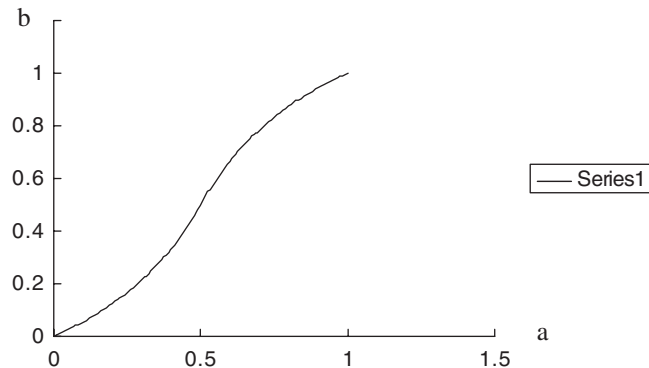


Figure 8. Relationship between true volume  $a$  and computed volume  $b$ .

from the free surface position. The relationship between  $a$  and  $b$  is shown in Figure 8 and can be expressed by the following fractional equation:

$$\begin{aligned}
 b &= 0.5 \left( \frac{1}{1-a} - 1 \right), & 0 \leq a < 0.5 \\
 b &= 0.5 \left( 3 - \frac{1}{a} \right), & 0.5 \leq a \leq 1
 \end{aligned}
 \tag{9}$$

Comparing the relationship between  $a$  and  $b$ , the error in this identification step is significant, especially around  $a=0.25$  and  $0.75$ . Correction of this error is needed and can be accomplished by using the above equation.

Function  $F$  for two-dimensional problems has the form

$$\begin{aligned}
 f(x, y) &= C_1 + C_2x + C_3y + C_5xy, & 0 \leq x \leq 1, & 0 \leq y \leq 1 \\
 C_1 &= F_{i,j} \\
 C_2 &= F_{i+1,j} - F_{i,j} \\
 C_3 &= F_{i,j+1} - F_{i,j} \\
 C_5 &= F_{i,j} - F_{i+1,j} - F_{i,j+1} + F_{i+1,j+1}
 \end{aligned}
 \tag{10}$$

When an  $F$  array set is provided to describe the liquid-wet area, a local partly filled sectional area can be distinguished by an equation,  $f=0.5$ , at every rectangle defined by four surrounding grid centers.

The arbitrary macro-shape of the interface could be reasonably described by composition of local segments produced by the above equation because of its curvy nature. Consider a circular section occupying a grid point only, with its center coinciding with the grid point center. The computed free surface curve and its section are shown in Figure 9(a). If the center of a circular section of the same size as the former is now at a rectangle corner as in Figure 9(b), the wet area does not appear at all from the equation of  $f=0.5$ .

For cases of circular section with a radius of multiplication similar to the grid size, the reproduced areas are smaller than the original areas (see Figure 10). The reproduced area relative to the

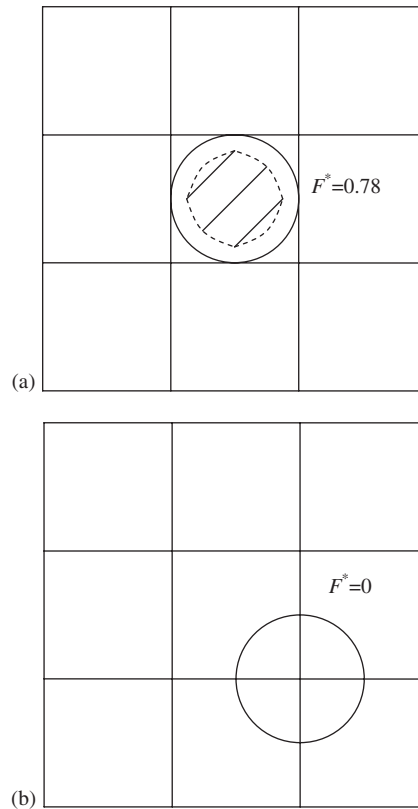


Figure 9. Errors produced from polynomial function in two-dimensional domain: diameter =  $\Delta x$ .

original area in a two-dimensional domain is shown in Figure 11. The ratio demonstrates that the reproduction ratio depends highly on the curvature of the section and the position of the center of the curvature. As the curvature radius grows, the slope of the reproduction area approaches 1. Similar to the one-dimensional case, the reproduction errors in the identification step are significant, especially when the curvature radius is small. The errors need to be treated in an appropriate way.

Once the true  $F^n$  array at a time step,  $n$ , is known, the free surface is identified by the previous polynomial function ((8)–(10)) in a three-, two-, or one-dimensional domain at a time step  $n$ , and the computed array at the same time step  $n$ ,  $F^{n,*}$ , is obtained with some identification errors:

$$E_{i,j}^n = F_{i,j}^n - F_{i,j}^{n,*} \tag{11}$$

The new array at the next time step,  $F^{n+1,*}$ , can be obtained from the same identification function for the previous time step by introducing a projection method. Assuming that the velocity fields vary linearly in space, we can find the position of the three-dimensional cube or two-dimensional rectangle or one-dimensional line segment by tracing backwards from the grid point of interest at the moment of interest, see Figure 11. The four  $F$  elements surrounding a rectangle are defined at the mesh cell centers. The position of each corner of the rectangle is found from the flow field

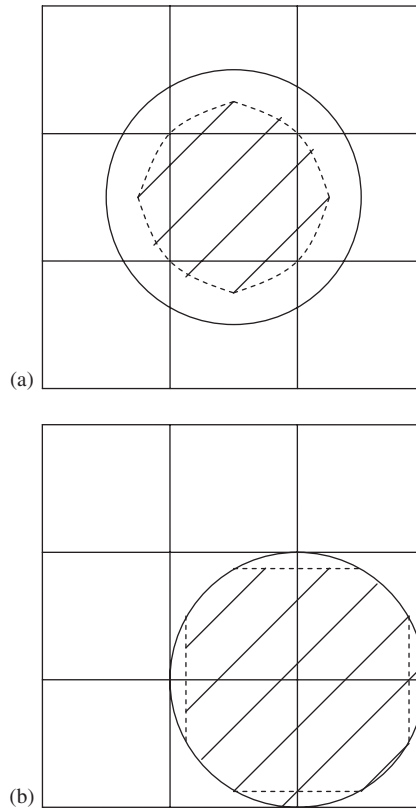


Figure 10. Errors produced from polynomial function in two-dimensional domain: diameter =  $2\Delta x$ .

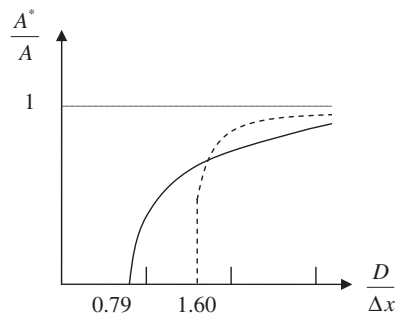


Figure 11. Error ratio *versus* diameter of circular section.

by tracing backward, an example of which is computed from the following equation:

$$\begin{aligned} \Delta x_{i,j} &= 0.5(U_{i-1,j}^n + U_{i,j}^n)\Delta t \\ \Delta y_{i,j} &= 0.5(V_{i,j-1}^n + V_{i,j}^n)\Delta t \end{aligned} \tag{12}$$

The velocity fields are assumed not to vary within a time increment. If the flow field is correctly provided, the fluid in the old cube (or rectangle or line segment) should automatically satisfy the continuity equation. If the CFL value is confined to less than or equal to 0.5 for convenience, then the old cube will position in the adjoining 27 grid points in a three-dimensional domain, or the old rectangle will be in the adjoining nine grid points in a two-dimensional domain, or the old line segment will be in the adjoining three grid points in a one-dimensional domain.

For example, looking at the two-dimensional problems, four  $F$  values are available at four grid centers in a large rectangle, and each  $f$  function is composed of four  $F$  values at four grid centers. The area occupied by liquid in one of the rectangles can be obtained by computing the sub-areas where  $f$  is greater than or equal to 0.5. The total computed liquid volume fraction or wet portion,  $F_{i,j}^{n+1,*}$ , can be obtained by adding the wet fractions in the four sub-areas. An example of the  $F$  value at the new time step,  $F_{i,j}^{n+1,*}$ , is graphically shown in Figure 12.

The error term of Equation (11) may primarily contribute to the total error during the identification step at both  $n$  and  $(n + 1)$  time steps; therefore, the error term at the following time step is approximated as identical to the error term at the previous time step under the assumption that the local curvature of the interface does not quickly rapidly so that a minor difference between the errors at the two time steps can be ignored. The new  $F_{i,j}^{n+1}$  value at grid point  $(i, j)$  is computed from the following equation:

$$F_{i,j}^{n+1} = F_{i,j}^{n+1,*} + E_{i,j}^n \tag{13}$$

The above equation for the  $F$  array at the new time step can include an  $F$  value larger than 1 or smaller than 0 due to the error correction step or the numerical computation of the volume projection in the reverse flow direction, including the numerical interpolation of the flow velocity field. The overflow or underflow is basically originated from the finite time increment. Overflow or underflow frequently occurs around the head or tail of a moving liquid body. Here we propose to truncate the overflow or underflow, and isotropically distribute the positive or negative excess amount to the adjoining partly filled grid points. The grid points for re-distribution of excess volume are chosen from the  $F$  matrix values, so that the cells chosen have the capacity to receive the excess volume. A few different combinations can happen depending on the  $F$  distribution

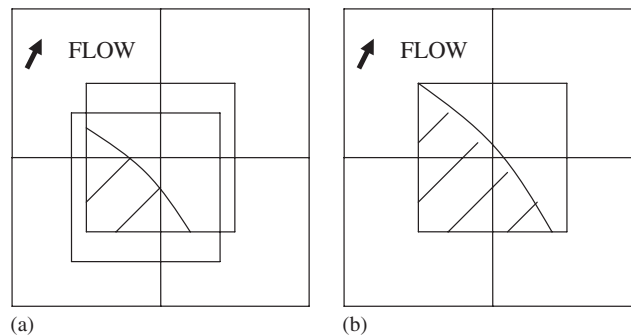


Figure 12. Graphical presentation of projection method to obtain new  $F_{i,j}^{n+1,*}$  for two-dimensional case.

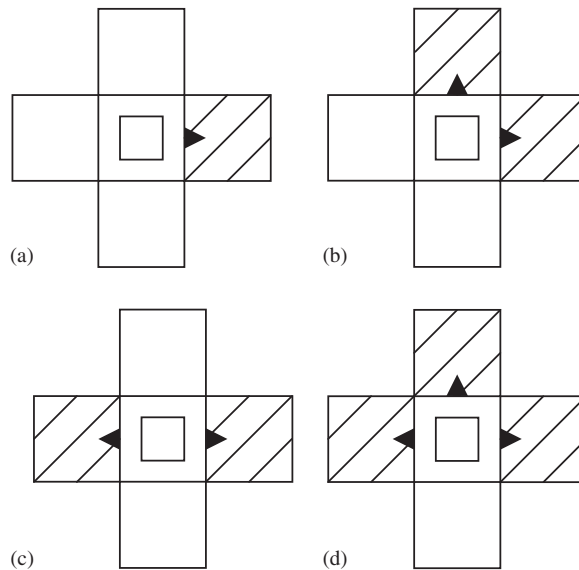


Figure 13. Re-distribution of overflow or underflow volume to adjoining grids.

around the overflow or underflow grid point in a two-dimensional domain, see Figure 13. This re-distribution step completes the whole computation of the movement of the free surface.

The present method is applied to several simple flow situations that have analytical solutions.

First, the method is tested for a one-dimensional flow case. The case has the following conditions: the horizontal velocity = constant and the time increment = 10% of CFL = 1.0 condition. The interface and liquid move in the  $x$  direction. The computed results coincide exactly with the analytical solution (see Test results).

Second, the method is evaluated for a two-dimensional flow case: a linear irrotational transition of a circular section in a direction parallel to the  $x$ -axis. The test conditions are the radius of the circular section = 3, 6, 9 times the horizontal grid size, respectively,  $U = 0.25$  m/s;  $\Delta x = \Delta y = 0.05$  m;  $\Delta t = 0.02$  s; total number of time steps = 120 to allow the initial circular section pass through a wall. Two properties are calculated to assess the accuracy of the method: the overall accuracy,  $H$ , and the relative net loss or gain of mass compared with the original mass,  $R$ .

The relative overall error,  $H$ , is computed by the following equation:

$$H = \frac{1}{A} \sum_j \sum_i (A_{i,j}^n - F_{i,j}^n)^2 \quad (14)$$

where the  $A_{i,j}$  array is the analytical solution of the given problem and  $n$  is the last computational time step. The relative volume change ratio,  $R$ , is obtained by

$$R = \left| \left( \frac{1}{A} \sum_j \sum_i F_{i,j}^n - 1 \right) \right| \quad (15)$$

3. TEST RESULTS

The computed  $F$  field for parallel advection of the section with radius of  $6\Delta x$  is shown in Figure 14. The computation errors of the present method and the donor-cell method relative to the analytical solution are shown in Table I.

The overall errors demonstrate that the PREC method is more accurate than the donor-cell method. The total volume error of the present method grows as the computation proceeds. The total volume was more accurately conserved with the present PREC method than with the donor-cell method. Figure 14 also demonstrates that the computed head speed with the present method is close to the analytical solution and that with the donor-cell method. Both results imply that the present method, PREC, produces a more accurate solution than the donor-cell VOF method for the examined cases.

A comparison of test results between the present method and donor-cell method for two-dimensional irrotational transition with an angle between  $0$  and  $45^\circ$  from the  $x$ -axis is shown in Table II, and the computed transition results for  $45^\circ$  are shown in Figure 15.

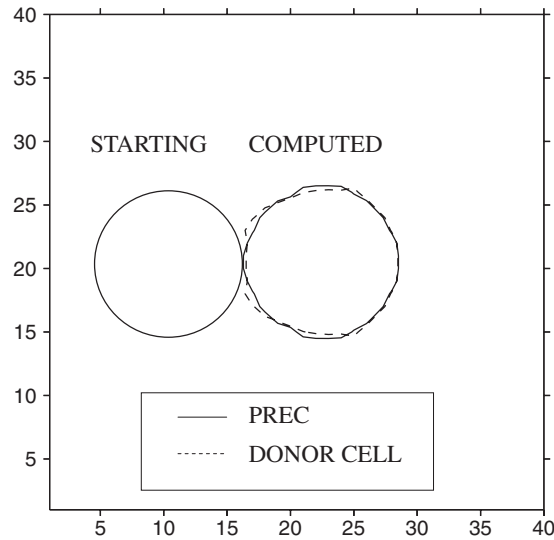


Figure 14. Comparison of present method and donor-cell method for horizontal transition case.

Table I. Errors of PREC method and donor-cell method for parallel transition cases.

	Method			
	PREC		Donor-cell	
Circle radius	Overall error, $H$	Volume error, $R$	Overall error, $H$	Volume error, $R$
$3\Delta x$	$6.84e-3$	$2.66e-4$	$2.36e-2$	$1.72e-4$
$6\Delta x$	$2.08e-2$	$7.69e-5$	$2.38e-2$	$4.33e-5$
$9\Delta x$	$3.97e-3$	$4.10e-6$	$1.57e-2$	$5.00e-7$

Table II. Errors of PREC method and donor-cell method for angled transition cases.

Angle (deg.)	Method			
	PREC		Donor-cell	
	Overall error, $H$	Volume error, $R$	Overall error, $H$	Volume error, $R$
0	$2.08e-2$	$7.69e-5$	$2.38e-2$	$4.33e-5$
22.5	$2.21e-2$	$3.62e-5$	$3.61e-2$	$3.87e-4$
45	$2.98e-3$	$4.95e-5$	$3.84e-2$	$1.10e-4$

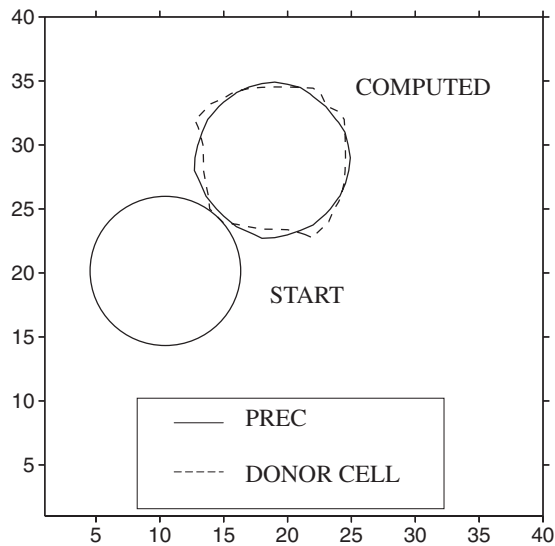


Figure 15. Comparison of present method and donor-cell method for sloped transition case.

It should be noted that computation errors of differing order are produced depending on the intersection angle between advection of fluid body and a reference axis. The difference may be explained with the repeated accumulation of advection errors in a fixed rectangular grid system for a specific angle. Similar to the earlier parallel transition cases, the PREC method provides more accurate solutions than the donor-cell method. Figure 15 also shows that the present method gives a smooth shape to the front part of the liquid body during advection, whereas the donor-cell method produces deformation around the front part.

Finally, the method is examined for the case of a pure rotation of fluid in a two-dimensional domain. The flow conditions are a constant angular velocity of  $\pi/6$  rad/s; the rotation center was the center of the circular liquid body;  $\Delta x = \Delta y = 0.05$  m;  $\Delta t = 0.09, 0.045, 0.03$  s; total number of time steps = 67, 133, 200 for circular section of radius of 3, 6, and 9 times the grid size, respectively. The total computation time corresponds to the half-cycle rotation time of the liquid body. The analytical solution for this case is the same as the initial condition. The computed final  $F$  contour for the rotation case is shown in Figure 16. The present method produces closer agreement with



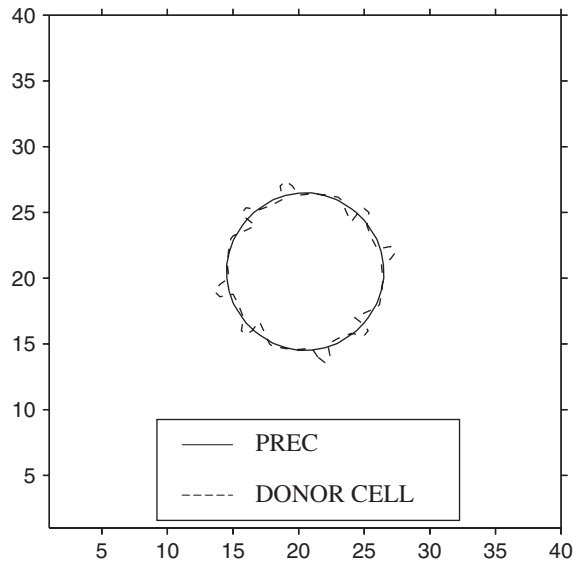


Figure 16. Comparison of present method and donor-cell method for rotational case.

Table III. Errors of PREC method and donor-cell method for rotating fluid cases.

Circle radius	Method			
	PREC		Donor-cell	
	Overall error, $H$	Volume error, $R$	Overall error, $H$	Volume error, $R$
$3\Delta x$	$1.32e-2$	$7.61e-4$	$9.24e-2$	$6.28e-4$
$6\Delta x$	$9.82e-3$	$5.12e-4$	$7.53e-2$	$6.24e-4$
$9\Delta x$	$2.56e-3$	$8.57e-4$	$7.21e-2$	$2.08e-3$

the analytical solution for section shape than the donor-cell method. The computed errors at the final step of the rotational flow cases are shown in Table III.

The computed overall errors and the volume conservation errors support that the present method gives more accurate solutions than the donor-cell method for the case of rotating flows.

#### 4. CONCLUSIONS

A new method, PREC, for free surface tracking has been proposed here. The method is composed of three steps: reconstruction step of the free surface using a polynomial function; computation of advection by using a projection method and additional adjustment to remove errors produced during the reconstruction step; and the truncating and redistribution of the overflow or underflow of  $F$  values to the adjoining grid points.

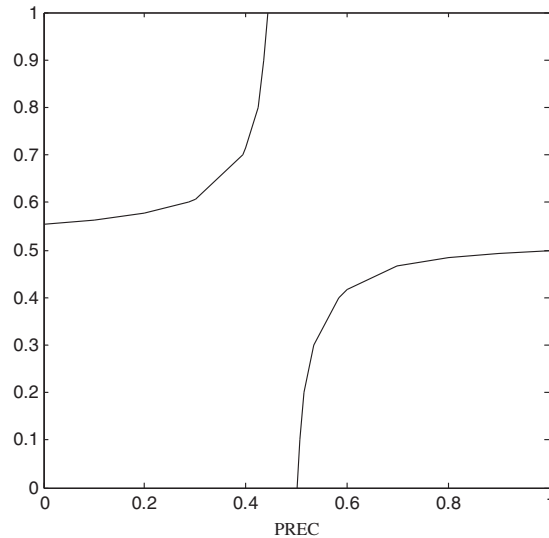


Figure 17. Comparison of present method and donor-cell method for rotational case.

The present third-order interpolation polynomial function for three-dimensional problems is reduced to a linear function when any two variables are fixed. Therefore, the present method could be thought of as an extension of a linear reconstruction method.

The PREC method shows reasonably accurate solutions, in general, with respect to the overall error, mass conservation, and the conservation of the frontal shape. The present method produces more accurate solutions than the donor-acceptor VOF method in the test runs presented. Conclusively, a comparison of results with analytical solutions confirm the applicability of the new method. Considering the importance of the head speed of a liquid body and the phase of the instantaneous fluid impact force exerted on a rigid body, the PREC method may be considered to reproduce the free surface movement in two-phase flows.

The present method is natural in the sense that the detailed function  $f$  perfectly matches with the coarse matrix  $F$  in the computational grid system. In general, the computations show that the present PREC method is useful for the simulation of free surface movement, especially when the free surface phases are important. When the free surface folds over or two or more free surfaces meet, the present model can deal with the problem with no difficulty. Another merit of the present method is that it includes some extreme cases, e.g. two free surfaces exist in a grid point, where the  $f$  contour looks like a saddle, see Figure 17, which is for a case of  $f(0, 0) = 0$ ,  $f(1, 0) = 1$ ,  $f(0, 1) = 0.9$ , and  $f(1, 1) = 0$ .

Extending the identification step to three-dimensional problems, errors will occur depending on the curvature radius and the position of the center of the curvature radius, similar to the two-dimensional problems. Further tests and applications for three-dimensional flow cases are needed in the future.

#### ACKNOWLEDGEMENTS

The present work was supported by Kookmin University (annual grant 2008) and POSCO E&C.

## REFERENCES

1. Lucy LB. Numerical approach to testing the fission hypothesis. *Astrophysical Journal* 1977; **82**:1013–1024.
2. Gingold RA, Monaghan JJ. Smoothed particle hydrodynamics: theory and application to non-spherical stars. *Monthly Notices of the Royal Astronomical Society* 1977; **181**:375–389.
3. Monaghan JJ, Gingold RA. Shock simulation by the particle method SPH. *Journal of Computational Physics* 1983; **52**:374–389.
4. Hirt CW, Amsden AA, Cook JL. An arbitrary Lagrangian–Eulerian computing method for all flow speeds. *Journal of Computational Physics* 1974; **14**:227–253.
5. Harlow FH, Welch JF. Numerical calculations of time-dependent viscous incompressible flow of fluid with free surface. *Physics of Fluids* 1965; **8**:2182–2189.
6. Amsden AA, Harlow FH. The SMAC method: a numerical technique for calculating incompressible fluid flow. *Los Alamos Scientific Laboratory Report, LA-4370*, 1970.
7. Hirt CW, Cook JL. Calculating three-dimensional flows around structures and over rough terrain. *Journal of Computational Physics* 1972; **10**:324–340.
8. Hirt CW, Nichols BD. Volume of fluid (VOF) methods for the dynamics of free boundaries. *Journal of Computational Physics* 1981; **39**:201–225.
9. Nichols BD, Hirt CW, Hotchkiss RS. SOLA-VOF: a solution algorithm for transient fluid flow with multiple free boundaries. *Los Alamos Scientific Laboratory Report No. LA-8355*, 1980.
10. Chorin AJ. Flame advection and propagation algorithm. *Journal of Computational Physics* 1980; **35**:1–11.
11. Chorin AJ. Curvature and solidification. *Journal of Computational Physics* 1985; **57**:472–490.
12. Partom IS. Application of the VOF method to the sloshing of a fluid in a partially filled cylindrical container. *International Journal for Numerical Methods in Fluids* 1987; **7**:535–550.
13. Jun L, Spalding DB. Numerical simulation of flows with moving interfaces. *Physicochemical Hydrodynamics* 1988; **10**:625–637.
14. Kothe DB, Mjolsness RC, Torrey MD. RIPPLE: a computer program for incompressible flows with free surfaces. *Los Alamos National Laboratory Report, LA-12007MS*, 1994.
15. Rider WJ, Kothe DB. Reconstruction volume tracking. *Journal of Computational Physics* 1998; **141**:112–152.
16. Kim MS, Lee WI. A new VOF-based numerical scheme for the simulation of fluid flow with free surface. Part I. New free surface-tracking algorithm and its verification. *International Journal for Numerical Methods in Fluids* 2003; **42**:765–790.
17. Sussman M, Smereka P, Osher S. A level set approach for computing solution to incompressible two-phase flows. *Journal of Computational Physics* 1994; **114**:146–159.
18. Sussman M, Almgren AS, Bell JB, Colella P, Howell LH, Welcome ML. An adaptive level set approach for incompressible two-phase flows. *Journal of Computational Physics* 1999; **148**:81–124.
19. Burchard P, Cheng LT, Merriman B, Osher S. Motion of curves in three spatial dimensions using a level set approach. *Journal of Computational Physics* 2001; **170**:720–741.
20. Muzaferija S, Peric M. Computation of free surface flows using interface tracking and interface capturing methods. In *Nonlinear Water Wave Interaction*, Chapter 2, Mahrenholtz O, Markewicz M (eds). WIT Press, Computational Mechanics Publications: Southampton, U.K., 1999.
21. Ubbink O. Numerical prediction of two fluid systems with sharp interface. *Ph.D. Thesis*, University of London, 1997.
22. Kim S-O, Sim Y, Kim E-K. A first-order volume of fluid convection model in three-dimensional space. *International Journal for Numerical Methods in Fluids* 2001; **36**:185–204.
23. Kim S-O, No HC. Second-order model for free surface convection and interface reconstruction. *International Journal for Numerical Methods in Fluids* 1998; **26**:79–100.
24. Du J, Fix B, Glimm J, Jia X, Li X, Li Y, Wu L. A simple package for front tracking. *Journal of Computational Physics* 2006; **213**:613–628.
25. Xiao F, Homma Y, Kono T. A simple algebraic interface capturing scheme using hyperbolic tangent function. *International Journal for Numerical Methods in Fluids* 2005; **48**:1023–1040.
26. Yabe T, Xiao F. Description of complex and sharp interface during shock wave interaction with liquid drop. *Journal of the Physical Society of Japan* 1993; **62**:2537–2540.